

# Plasma Shape Effects on Geodesic Acoustic Oscillations

L. Villard\*, P. Angelino\*, A. Bottino<sup>†</sup>, R. Hatzky\*\*, S. Jolliet\*,  
B.F. McMillan\*, O. Sauter\* and T.M. Tran\*

\**Centre de Recherches en Physique des Plasmas, Association Euratom - Confédération Suisse, EPFL, 1015 Lausanne, Switzerland*

<sup>†</sup>*Max-Planck Gesellschaft Institute for Plasma Physics, D-85748 Garching, Germany*

\*\**Computer Center of the IPP and the Max-Planck Gesellschaft, D-85748 Garching, Germany*

**Abstract.** Geodesic acoustic mode (GAM) [1] oscillations in tokamak plasmas are known to be sensitive to the value of the safety factor  $q$ . Through its linear and nonlinear interactions with ITG turbulence it has recently been shown in direct numerical global simulations [2] that the turbulence driven heat transport is larger when GAM oscillations of large amplitude are present, resulting in an anomalous transport scaling with the inverse plasma current. GAM dispersion relations have been derived for circular, large aspect ratio configurations, and, recently, for helical configurations [3]. Linear simulation results are presented using the global, PIC, finite element codes GYGLES [4] and ORB5 [5] for the GAM frequency, damping rate and Rosenbluth-Hinton [6] residual zonal flow for a scan in plasma elongation. It is found that GAM frequency slightly decreases, while GAM damping rate and residual zonal flows increase with elongation. Nonlinear ITG simulations using the ORB5 code [5] show that elongation reduces heat transport and that this is related to the plasma current and not  $q$  alone.

**Keywords:** turbulence, geodesic acoustic modes, ITG modes, tokamak

**PACS:** 52.30.Gz, 52.35.Qz, 52.35.Mw, 52.35.Ra

## ITG TURBULENCE, ZONAL FLOWS AND GAMS

Ion Temperature Gradient (ITG) driven turbulence is known to interact with axisymmetric  $\mathbf{E} \times \mathbf{B}$  flows [7]. These flows can be nonlinearly generated by ITG modes. They in turn tend to reduce the ITG turbulence level by their shearing action on the elongated structures of toroidal ITG modes. When the  $\mathbf{E} \times \mathbf{B}$  zonal flow shearing rate is comparable to the turbulence decorrelation time the modes are stabilised. The main consequence is a substantial reduction in the anomalous, turbulence driven radial transport.

Axisymmetric  $\mathbf{E} \times \mathbf{B}$  flows exist in two branches, linearly speaking. A zero frequency branch (zonal flows, ZF) and a finite frequency branch (GAM) [1]. The GAM is damped by collisionless kinetic effects. The GAM component of the  $\mathbf{E} \times \mathbf{B}$  flows is less effective than the stationary ZF component to suppress turbulence [8]. On the other hand, the zonal flows have a completely undamped component [6]: when an initial  $\mathbf{E} \times \mathbf{B}$  perturbation is applied to the system, the residual is given by

$$v_{\mathbf{E} \times \mathbf{B}}(t \rightarrow \infty)/v_{\mathbf{E} \times \mathbf{B}}(t = 0) = \left(1 + 1.6q^2/\varepsilon^{1/2}\right)^{-1}. \quad (1)$$

Hence the general idea: in order to reduce the turbulence level, and possibly the anomalous transport, situations in which GAMS are damped and residual steady zonal flows

are high should be favourable. GAM properties depend on the safety factor value  $q$ . Its frequency and damping rate are

$$\omega_{\text{GAM}}^2 = 2 \frac{c_s^2}{R^2} \left( 1 + \frac{1}{2q^2} \right) \quad \gamma_{\text{GAM}}/\omega_{\text{GAM}} \approx \exp(-q^2 - 1/2). \quad (2)$$

The effect of  $q$  has been observed in nonlinear simulations: the stationary or oscillatory nature of axisymmetric flows depends critically on the  $q$  value [9]. Recently, direct numerical simulations (in the absence of input power) have shown that the ITG turbulent heat flux scales inversely proportional to the total plasma current, and that the ratio of oscillatory (GAM) to quasi-steady (ZF) amplitudes scales in the same way [2], suggesting that this type of physics is responsible for the scaling.

Little is known [3] about the effect of plasma cross-section shaping on the GAM, ZF and ITG behaviour. This paper presents a study of the effect of plasma elongation on the linear GAM spectrum and nonlinear ITG turbulence.

## MODEL

In order to ensure a correct calculation of zonal flow damping [6] the gyrokinetic description is used. Here we assume gyrokinetic ions and an adiabatic electron response on magnetic surfaces. The model is global and no geometrical approximation is made (besides the numerical discretization). The magnetic configuration consists in toroidal axisymmetric, low  $\beta$ , ideal MHD equilibria computed with the CHEASE code [10]. The global, nonlinear, gyrokinetic ORB5 code [5] is used. The perturbed potential is represented with 3D cubic B-spline finite elements. The perturbed ion distribution function is discretized with marker particles (PIC,  $\delta f$  method). Numerical statistical noise coming from the PIC representation is reduced with the “optimized loading” scheme [11] and through field-aligned Fourier filtering of unphysical, small parallel wavelength components that break the gyrokinetic ordering. The equilibrium distribution function  $f_0$  is a canonical Maxwellian, i.e. a true equilibrium in the gyrokinetic sense:  $df_0/dt|_0 = 0$ , in other words it is constant along unperturbed characteristics. This choice was devised in order to avoid spurious GAM excitation [12]. More details can also be found in [13]. The ORB5 code can be run in linear mode and compared to the GYGLES code [4].

## LINEAR GAM BEHAVIOUR WITH ELONGATION

We start the investigations by prescribing an initial density perturbation and computing the linear response of the system. We define a sequence of equilibria of varying elongation from  $\kappa = 1.0$  to  $\kappa = 2.5$ , keeping the aspect ratio  $R/a = 6$ , the safety factor on axis  $q_0 = 1.23$ , and using the same toroidal current density profile prescription as a function of the radial coordinate  $s = \sqrt{\psi/\psi_a}$ , where  $\psi$  is the poloidal magnetic flux. This profile results in a monotonic  $q$  profile. The edge  $q$  value changes with elongation from  $q_a = 3.1$  for  $\kappa = 1.0$  to  $q_a = 6.26$  for  $\kappa = 2.5$ , while the value of  $q$  at mid radius changes only slightly, from  $q(0.5) = 1.43$  for  $\kappa = 1.0$  to  $q(0.5) = 1.46$  for  $\kappa = 2.5$ . The normalised plasma current,  $I_N = I[\text{MA}]/a[\text{m}]B[\text{T}]$ , is nearly proportional to  $\kappa$ , varying

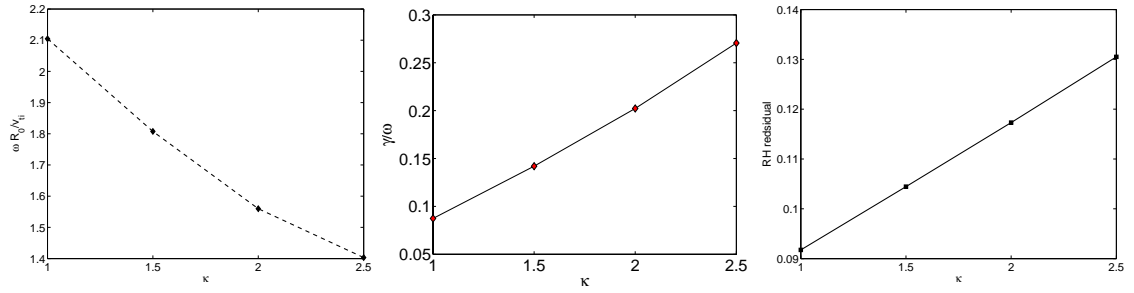


**FIGURE 1.** Frequency (left), damping rate (middle) and undamped zonal flow residual (right) versus plasma elongation computed from the linear response to an initial axisymmetric density perturbation. Only the  $(m = 0, n = 0)$  Fourier component of the perturbed density has been kept in these simulations.

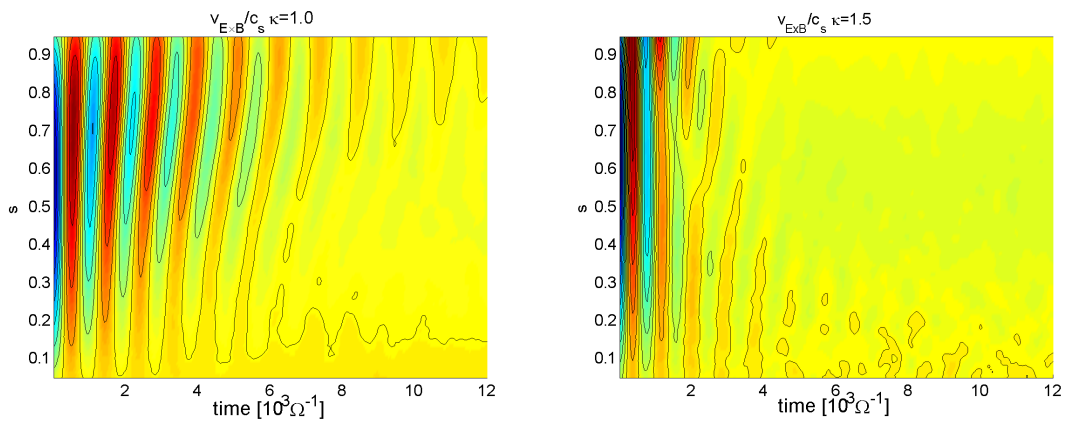


**FIGURE 2.** Contour plots of  $v_{E \times B}$  versus time (horizontal axis) and radius (vertical axis), for an initial given density perturbation. Left:  $\kappa = 1.0$ , with  $m = 0, n = 0$  only kept. Right:  $\kappa = 1.5$ , with poloidal sidebands included  $m \in [-4, +4]$ . The stronger damping of GAM oscillations for the elongated case is clearly visible.

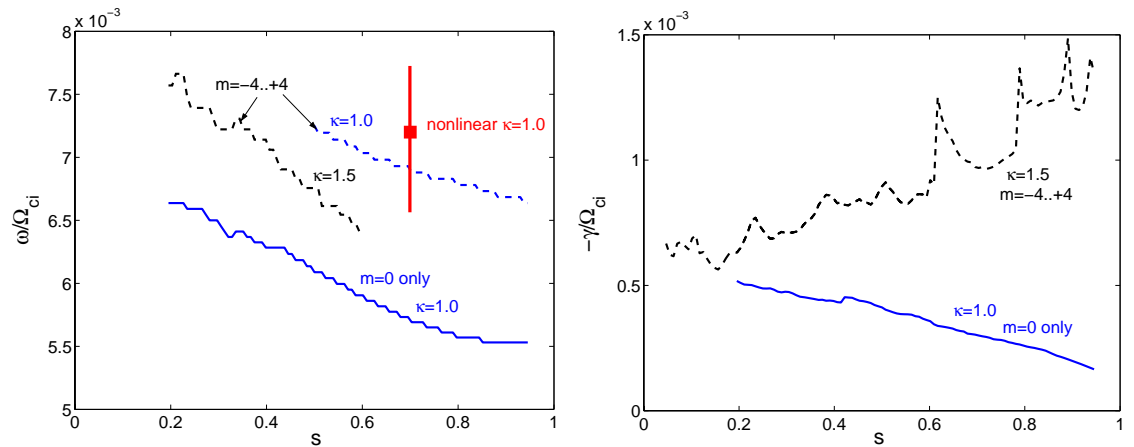


**FIGURE 3.** Frequency (left) and damping (right) of GAMs versus minor radius coordinate  $s$  for circular ( $\kappa = 1.0$ ) and elongated ( $\kappa = 1.5$ ) cases. The square with the vertical bar indicates the frequency of oscillations observed in nonlinear simulations.

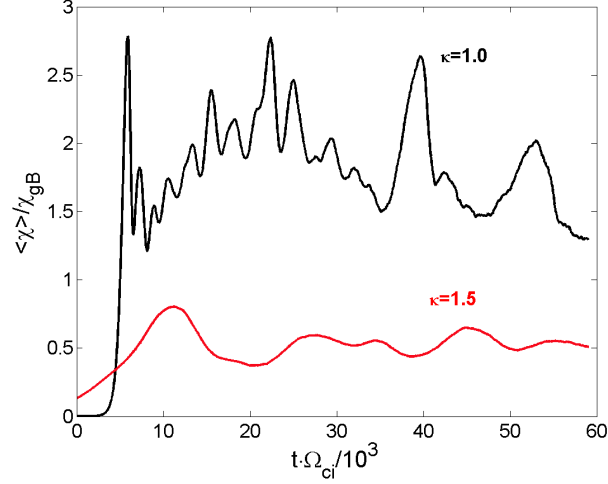


**FIGURE 4.** Averaged heat diffusivity in gyro-Bohm units versus time for  $\kappa = 1.0$  and  $\kappa = 1.5$ .

from  $I_N = 0.284$  for  $\kappa = 1.0$  to  $I_N = 0.757$  for  $\kappa = 2.5$ . Nearly force-free equilibria are used, so that Shafranov shift effects are negligible.

The frequency, damping rate and residual undamped zonal flow are obtained from a fit of  $\int_0^1 \phi_{00}(s, t) ds$  signals. The results are plotted in Figure 1. The real frequency decreases with elongation; note that the analytical result for the GAM frequency, obtained for circular, large aspect ratio [1], would be  $\omega = 2$  in the units of Figure 1 (left). Most interestingly, the damping rate increases roughly proportionally to the elongation. The ZF residual shows a slight increase with  $\kappa$ .

In order to analyze the GAM behaviour in more detail, we focus on two cases: circular ( $\kappa = 1.0$ ) and moderately elongated ( $\kappa = 1.5$ ). Simulations including the poloidal sidebands  $m \in [-4, +4]$  are performed in order to study geometrical coupling effects. We also examine the radial ( $s$ ) dependence of GAM oscillations and try to distinguish  $q$  profile effects from elongation effects. Figure 2 shows time and radial contours of the  $\mathbf{E} \times \mathbf{B}$  velocity for the circular case (left) and the elongated case (right). In the circular plasma, the lower damping and slightly lower frequency at large  $s$ , where  $q$  is larger, is visible. This is in agreement with analytical expressions Eqs.(2,??). The elongated case has a much larger GAM damping rate. These results are summarized in Figure 3, in which the frequency observed in nonlinear simulations is indicated by the square, indicating that these correspond to the excitation of GAMs.

## NONLINEAR GLOBAL SIMULATIONS

Using the same equilibria as in the previous Section, we now turn to the investigation of the nonlinear ITG - ZF - GAM behaviour. The parameters are chosen similar to the CYCLONE base case [14], with the exception of the use of ideal MHD equilibria with  $R/a = 6$ ,  $\kappa = 1.0$  and  $\kappa = 1.5$ . The ORB5 code is used [5] with the following numerical parameters. The grid resolution is  $N_s \times N_\theta \times N_\varphi = 128 \times 320 \times 256$ . The

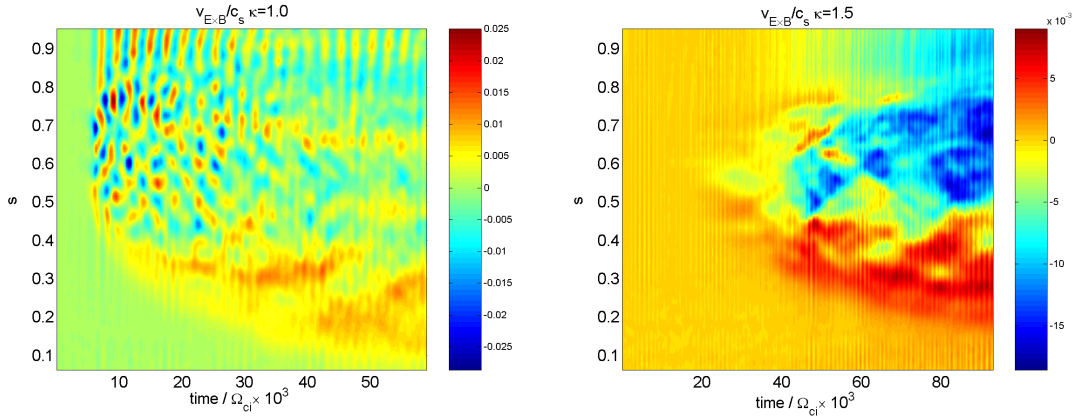


**FIGURE 5.** Contours of the  $\mathbf{E} \times \mathbf{B}$  velocity versus radius and time, for the circular (left) and elongated (right) cases. The GAM oscillations are much more pronounced, and the quasi-steady ZF component much less, for the circular case than for the elongated case.

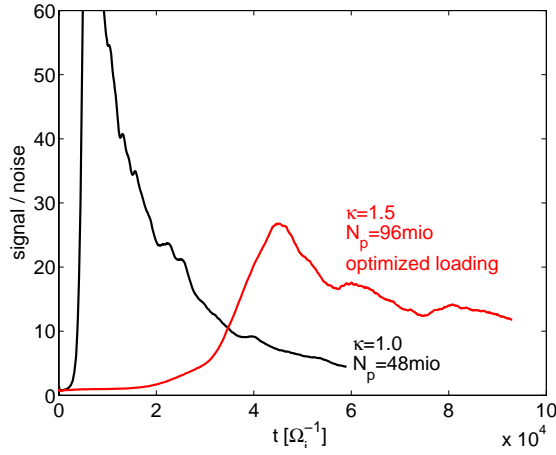


**FIGURE 6.** Signal to noise ratio for the nonlinear simulations shown in Figures 4-5.

number of marker particles is  $N_p = 48 - 96 \times 10^6$ . A field-aligned Fourier filter with  $\Delta m = 5$  is applied; this has been checked to be in agreement with gyrokinetic ordering. The number of modes is thus  $N_s N_{(m,n) \in \text{filter}} = 180000$ , and the number of particles per mode is  $266 - 532$ , which has proven to be sufficient for numerical noise suppression and large enough to yield close to converged results [15]. In addition, optimisations of marker particle loading [11] are performed.

The time evolution of the averaged heat diffusivity normalized to the gyro-Bohm diffusivity  $\chi_{gB} = \rho_s^2 c_s / a$  is represented in Figure 4, for both the circular and elongated cases. The large reduction (a factor of about 3) in radial heat transport for the  $\kappa = 1.5$  case can be attributed, as least in part, to a reduction in the linear drive. The initial temperature profiles are identical as function of  $\psi$ , which means that the averaged spatial gradient is lower for the elongated case, while being identical on the equatorial plane. The stronger drive of the circular case manifests itself in the presence of bursts in the

heat flux, which are practically absent in the elongated plasma. Part of the reduction in heat transport may be attributable to a difference in zonal flows and GAM behaviour. Figure 5 shows contours of the  $\mathbf{E} \times \mathbf{B}$  velocity versus radius and time. The quasi-steady part of the  $\mathbf{E} \times \mathbf{B}$  flow is stronger for the elongated case, while GAM oscillations are much more apparent for the circular case. Qualitatively, the nonlinear results are thus consistent with the findings of the linear GAM behaviour: elongation increases GAM damping rate. Finally, Figure 6 shows the numerical statistical signal to noise ratio

$$\frac{\sum_{(m,n) \in \text{filter}} |\delta n_{(m,n)}|^2 / N_{mn}}{\sum_{(m',n') \notin \text{filter}} |\delta n_{(m',n')}|^2 / N_{m'n'}}. \quad (3)$$

The main conclusion of the paper is thus that elongation is favourable for energy confinement time. This is due to both a reduction in linear ITG drive and an increase in GAM damping. These results are consistent with a scaling of confinement time increasing with normalized plasma current. This also shows that the safety factor  $q$  alone is not the only important parameter: indeed, the elongated equilibrium studied here has even a higher  $q_a$  than the circular one, which would yield, if  $q$  value effects were alone responsible, a larger heat flux than the circular case. More work is necessary in order to better distinguish the relative roles of linear ITG drive and GAM behaviour in order to possibly identify an intrinsic effect of plasma elongation.

## ACKNOWLEDGMENTS

Computations were performed on the IBM Blue Gene / L and Pleiades-2 clusters of the EPFL. Work supported in part by the Swiss National Science Foundation.

## REFERENCES

1. N. Winsor, L.J. Johnson and M.J. Dawson, *Phys. Fluids* **11**, 2448 (1968).
2. P. Angelino, A. Bottino, R. Hatzky, S. Jolliet, O. Sauter, T.M. Tran and L. Villard, *Plasma Phys. Controlled Fusion* **48**, 557-571 (2006).
3. H. Sugama and T.H. Watanabe, *Phys. Plasmas* **13**, Art.No. 012501 (2006).
4. M. Fivaz, S. Brunner, G. De Ridder, et al., *Computer Phys. Commun.* **111**, 27 (1998).
5. T.M. Tran, K. Appert, M. Fivaz, et al., *Theory of Fusion Plasmas*, International Workshop, Varenna, Italy, August-September 1998, ISPP-18, edited by J.W. Connor, E. Sindoni and J. Vaclavik (Editrice Compositori, Bologna, 1999), pp. 45-58. S. Jolliet et al., this Workshop.
6. M.N. Rosenbluth, F.L. Hinton, *Phys. Rev. Lett.* **80**, 724 (1998)
7. P.H. Diamond, S.I. Itoh, K. Itoh and T.S. Hahm, *Plasma Phys. Controlled Fusion* **47**, R35 (2005).
8. T.S. Hahm, et al., *Phys. Plasmas* **6**, 922 (1999).
9. N. Miyato and Y. Kishimoto, *Phys. Plasmas* **11**, 5557 (2004).
10. H. Lütjens, A. Bondeson and O. Sauter, *Comput. Phys. Commun.* **97**, 219 (1996).
11. R. Hatzky, et al., *Phys. Plasmas* **9**, 988 (2002).
12. Y. Idomura, S. Tokuda and Y. Kishimoto, *Nucl. Fusion* **43**, 234 (2003).
13. P. Angelino, A. Bottino, R. Hatzky, S. Jolliet, O. Sauter, T.M. Tran and L. Villard, *Phys. Plasmas* **13**, no.052304 (2006).
14. A.M. Dimits, et al., *Phys. Plasmas* **7**, 969 (2000).
15. A. Bottino, et al., 33rd European Physical Society Conference on Plasma Physics, (Rome, Italy, June 19-23, 2006) paper No. O3.001.